Observations of Europa's Tenuous Atmosphere

M. A. McGrath
NASA Marshall Space Flight Center

C. J. Hansen and A. R. Hendrix
Jet Propulsion Laboratory

ABSTRACT

Europa is known to possess a predominantly molecular oxygen atmosphere produced by sputtering of its icy surface. This atmosphere, which is diagnostic of surface composition and processes, has been characterized by Hubble Space Telescope, Galileo, Cassini and ground-based observations. The primary means of detecting Europa's atmosphere is via emission from the atomic constituents. The relative strengths of the atomic oxygen emission lines allow inference of a dominant O_2 component. Oxygen, sodium and potassium are known minor constituents. A relatively dense ionosphere has also been detected on several occasions by Galileo radio occultation measurements, the presence of which appears to require a sunlit trailing hemisphere. Neither the spatial distribution of the oxygen emission associated with the atmosphere, nor the obvious variability of the atmospheric emissions and the ionospheric densities, has been adequately explained to date.

1. INTRODUCTION

Europa is one of a growing cadre of solar system objects that possess very tenuous atmospheres (often called exospheres), which are characterized by a collisionless gas with exobase at the surface. Their discovery - at Mercury, the Moon, Io, Europa, Ganymede, Callisto, Enceladus, Triton, Pluto - has become common in recent years because of the increasing sophistication of remote sensing and in situ observing techniques. They are produced by a wide variety of physical processes, including sublimation, sputtering (by both photons and charged

particles), micrometeroid bombardment, geyers and volcanoes. This class of atmosphere is important because of the often unique information they can provide about the environment of the satellite (which has implications for understanding the magnetospheres of the parent planets), surface processes, and therefore, potentially, about interior and surface compositions of these bodies. Although tenuous, these exospheres also produce measurable ionospheres with peak densities of ~$10^3 - 10^4$ cm^{-3}, which were one of the first definite indications of the presence of atmospheres associated with these bodies (e.g., *Kliore et al.* 1974, 1975).

The idea that the Galilean satellites might possess tenuous atmospheres, and that satellites with atmospheres could possess neutral tori, began to be explored in earnest in the early 1970s with a series of important milestones. Water ice was positively identified on the surfaces of Europa, Ganymede and Callisto by *Pilcher et al.* (1972). An approximately 1μbar atmosphere was reported on Ganymede from a stellar occultation measurement (*Carlson et al.*, 1973). *McDonough and Brice* (1973) suggested that, as a consequence of their atmospheres, there might be neutral clouds of orbiting atoms associated with Titan and the Galilean satellites because most material removed from the atmospheres does not attain escape velocity. Detection of hydrogen (*Judge and Carlson,* 1974), sodium (*Brown,* 1974), and potassium (*Trafton,* 1975) clouds associated with Io seemed to confirm these early expectations. Pioneer 10 observations of Europa made in 1973 using the long wavelength channel ($\lambda < 1400$ Å) of the UV photometer were first reported as a null result (*Judge et al.,* 1976), but subsequently reported as a detection of oxygen at Europa using the short wavelength ($\lambda < 800$ Å) UV photometer channel (*Wu et al.,* 1978). Around this time the Io plasma environment also began to be characterized (*Frank et al.,* 1976; *Kupo et al.,* 1976). The realization that Europa, like Io, is immersed in and impacted by a high flux of particles that could dissociate and sputter water ice (*Brown et al.,* 1977), made the

possibility of a tenuous atmosphere and extended neutral clouds associated with Europa seem much more plausible.

The *Carlson et al.* (1973) detection motivated *Yung and McElroy* (1977) to develop a photochemical model of a sublimation-driven water ice atmosphere. Because the hydrogen preferentially escapes, such an atmosphere evolves into a stable molecular oxygen atmosphere by photolysis of H_2O. In their model, nonthermal escape of O atoms balances the production of O_2 to yield a surface pressure of ~1μbar, consistent with the *Carlson et al.* result. They concluded that Ganymede should have an appreciable oxygen atmosphere and ionosphere, but that the higher albedo of Europa would inhibit sublimation, suppressing the formation of O_2. Based on laboratory data, *Lanzerotti et al.* (1978) suggested that bombardment of the satellite surfaces by the jovian plasma leads to an erosion rate on Ganymede that could support the H_2O partial pressure used by *Yung and McElroy* (1977), and that the rates would be much larger at Europa. Subsequent laboratory data showed that O_2 is directly produced in and ejected from water ice (*Brown et al.*, 1980), a process referred to as radiolysis. When the Voyager 1 Ultraviolet Spectrometer stellar occultation measurements of Ganymede yielded an upper limit on surface pressure of 10^{-5}μbar (*Broadfoot et al.,* 1979), *Kumar et al.* (1982) pointed out that the *Yung and McElroy* model possessed an additional stable solution with a much lower surface pressure of ~10^{-6} μbar, compatible with the Voyager 1 result.

Finally, using the laboratory sputtering data of *Brown et al.* (1980), *Johnson et al.* (1982) estimated that O_2 sputtered from water ice on Europa could yield a bound atmosphere with a column density of ~ (2-3) x 10^{15} cm^{-2}. Since O_2 does not stick efficiently at Europa temperatures and does not escape efficiently, the atmosphere is dominated by O_2 even though the sputtered flux of H_2O molecules is larger than that of O_2. This early work set the stage for the successful detection of oxygen at Europa, which we describe in detail below.

Generally speaking, Europa's tenuous atmosphere is produced by radiolysis and sputtering of its icy surface, with a minor contribution from sublimation of water ice. As pointed out by Johnson (2002)**,** Europa is an example of a surface bounded atmosphere. Once products are liberated from the surface, the diatomic species (primarily O2, but to a lesser extent H2) are expected to become the dominant ones because they are non-condensible, neither sticking or reacting efficiently with the surface and therefore accumulating in the atmosphere but becoming thermalized through repeated surface encounters. The other water group species are lost either by direct escape because they are light, or by sticking to or reacting with the surface. A summary of the observations pertinent to Europa's atmosphere acquired to date is provided in Table 1. Figure 1 illustrates schematically the species detected, and the range of altitudes over which the

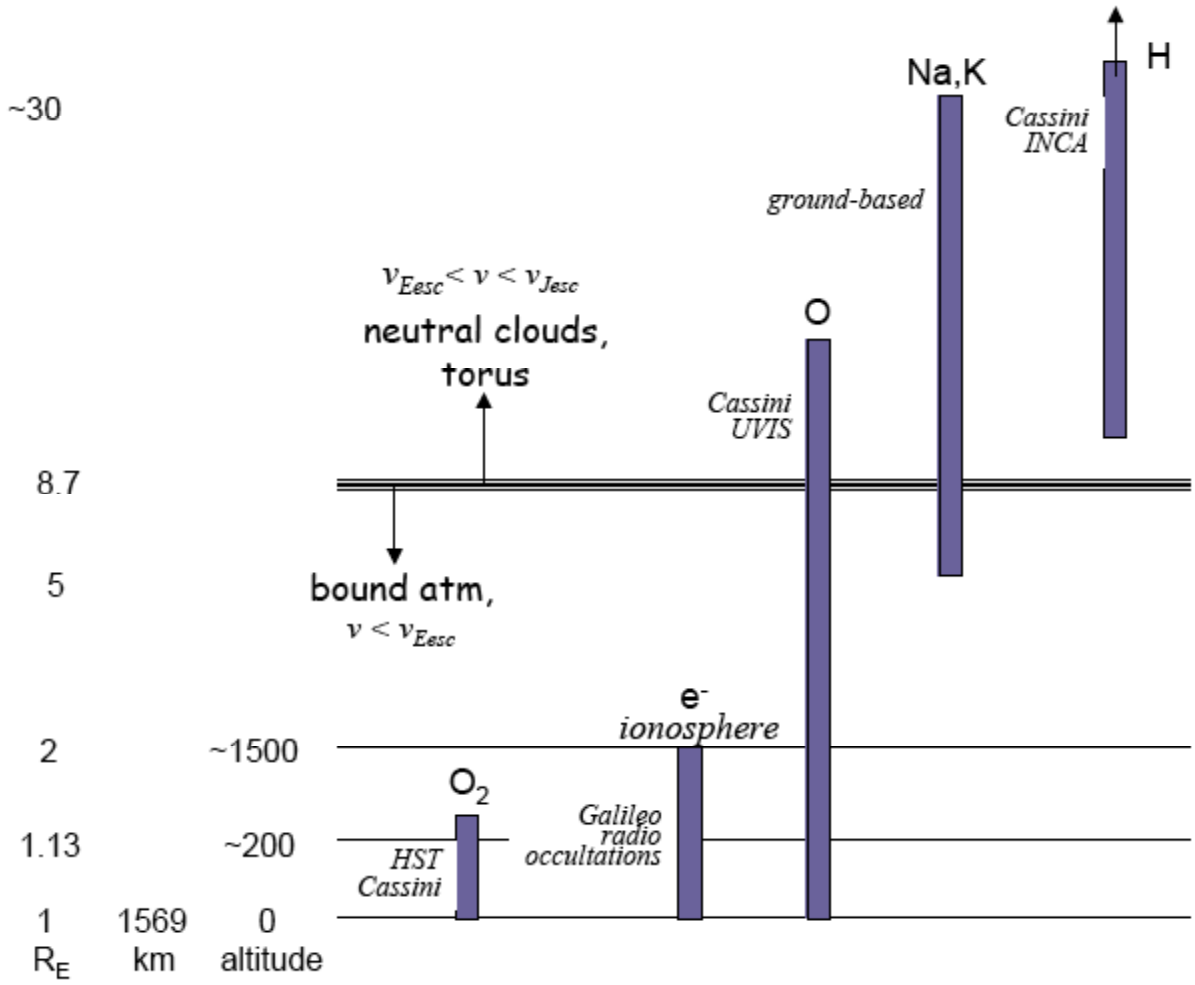

Figure 1. *Schematic diagram showing the constituents detected in Europa's tenuous atmosphere, and the regions in which they have been observed. Generally speaking the bound atmosphere is defined by the region within which Europa's gravity dominates, at* $r \leq 8.7\ R_E$, *where the velocity of the constituents is less than Europa's escape velicity* (v_{Eesc}) *of ~ 2 km/sec. Beyond this region, particles either escape from Jupiter altogether* ($v > v_{Jesc}$), *or enter orbit around Jupiter as clouds or a torus near Europa's orbital distance. [1* R_E *= 1569 km]*

detections have been made, where 1 Europa radius (R_E) is 1569 km. It is important to note that the various observations span quite different regimes of the atmosphere, neutral clouds, and torus. In particular, observations of the main constituent of the atmosphere, O_2, and observations of the minor species, Na and K, have no overlap. A rough boundary between the bound atmosphere and neutral clouds is the radius of the Lagrange sphere of Europa, which occurs at ~8.7 R_E. Inside this boundary, Europa's gravitational field dominates Jupiter's; outside this boundary the opposite is true. We discuss the various observations roughly in order of increasing distance from Europa's surface, considering first the bound O_2 atmosphere, which has a scale height of roughly a hundred kilometers.

We concentrate in this chapter on providing detailed descriptions of the observations made to date of Europa's tenuous atmosphere. The following chapter by *Johnson et al.* provides a complimentary review of the detailed interpretations and modeling these observations have spawned. It includes an in-depth discussion of the wide range of physical characteristics that can be gleaned about Europa and its environment from these observations. We focus here on providing a clear explanation of the quality and limitations of the existing observations and data, and on providing descriptions of the simple models presented in the observational papers required to derive basic quantities such as column densities from the observations. Where possible we provide further details about and new presentations of previously published data. Finally, we summarize outstanding issues, and provide recommendations for future observations that may be helpful in resolving them.

2. OXYGEN ATMOSPHERE

The major constituent of Europa's tenuous atmosphere is now known to be molecular oxygen, which has been inferred via detection of ultraviolet (UV) line emission from atomic oxygen. Emission from neutral atmosphere constituents are overwhelmed by reflected sunlight at visible wavelengths, whereas at UV wavelengths most planetary bodies have albedos more than an order of magnitude lower than in the visible. Ten sets of ultraviolet observations of Europa now exist, six made with the Earth-orbiting Hubble Space Telescope (HST), three made with the Cassini spacecraft, and one made with the New Horizons spacecraft. The specifics of the observations are summarized in Table 1. The HST and New Horizons observations acquired in February 2007 are still proprietary, but preliminary results have been presented recently by *Retherford et al.* (2007). The HST observations made in April 2007 are still proprietary, with no results yet available.

2.1 Hubble Space Telescope Observations

The first unambiguous detection of Europa's atmosphere was made by *Hall et al.* (1995) in June 1994 using HST's Goddard High Resolution Spectrograph (GHRS) with a 1.74´´ x1.74´´ slit centered approximately on Europa's trailing hemisphere. They discovered emission from the semi-forbidden and optically allowed oxygen multiplets OI($^5S^o$ - ^3P)1356 Å and OI($^3S^o$ - ^3P)1304 Å (bottom panel of Figure 1). In these and subsequent observations of the UV oxygen emission multiplets there are several contributors to the emission, and several possible sources:

(1) solar resonance fluorescence scattering by O atoms in the Earth's atmosphere

(2) solar emission line and continuum photons reflected from the surface of Europa

(3) solar resonance fluorescence scattering by O atoms in Europa's atmosphere

(4) electron impact excitation of oxygen, $e^- + O \rightarrow O^* \rightarrow O + \gamma$

(5) electron impact dissociative excitation of O_2, $e^- + O_2 \rightarrow O^* \rightarrow O + \gamma$

The *Hall et al.* observations were performed in Earth shadow, where the contribution from (1) is

minimal; such background emission would fill the slit, and produce flat-topped emission line profiles, which was not observed. Figure 1 shows that in addition to the oxygen emissions, emission from CII 1335 A is also detected; it is produced by process (2). Although the reflectivity with wavelength is unknown in the UV for Europa, if it is assumed to be constant with wavelength, the CII emission can be used to estimate the contribution to the oxygen emissions from process (2). Modeling the CII emission as reflected sunlight allows a derivation of the reflectivity of Europa at this wavelength, which was found to be 1.6 ± 0.5 % (*Hall et al.,* 1998). The contribution to the spectrum from process (2) is shown in Figure 1 as a solid line underlying the observed spectrum. It is not a significant contributor to the OI 1356 emission line, which is a semi-forbidden transition, because the sun does not produce line emission at this wavelength. *Hall et al. (*1995, 1998) showed that process (3) produces a negligibly small contribution to the oxygen emissions at Europa.

The inference that process (5) dominates over process (4), and that Europa's atmosphere is predominantly O_2 and not O, is based on the ratio of the 1356 Å to 1304 Å emission intensities, I(1356)/I(1304). For the June 1994 observations, this ratio is ~1.9:1, after accounting for the contribution from processes (2) and (3). For a Maxwellian distribution of electrons over a broad energy range this intensity ratio is 2, based on the electron impact cross sections of *Noren et al.* (2001). By contrast, using the OI 1304 Å cross section of *Doering et al.* (2001), the I(1356)/I(1304) ratio for O atoms has a broad maximum of 0.35 at 4 eV. A molecular oxygen atmosphere with column density 1.5 ± 10^{15} cm^{-2} ($P_o = 2.2 \pm 0.7 \times 10^{-6}$ μbar) was inferred for the trailing hemisphere of Europa, which is consistent with the early estimate of a bound atmosphere by *Johnson et al.* (1982) and the low pressure solution discussed by *Kumar et al.* (1982). In deriving the O_2 column density, *Hall et al*. (1995) assumed: the spatial distribution of Europa's atmosphere is confined to the geometric cross section of the observed hemisphere (i.e., the scale

height of the atmosphere is significantly smaller than the radius of Europa); a negligible contribution to the observed flux is emitted from above the tangential limb along the terminator; the Io plasma torus electrons responsible for exciting the observed emissions interact with the atmosphere without energy degradation; and no electrodynamic, sub-Alfvenic interactions such as observed by Voyager at Io (e.g., *Ness*, 1979, *Neubauer*, 1980) were considered.

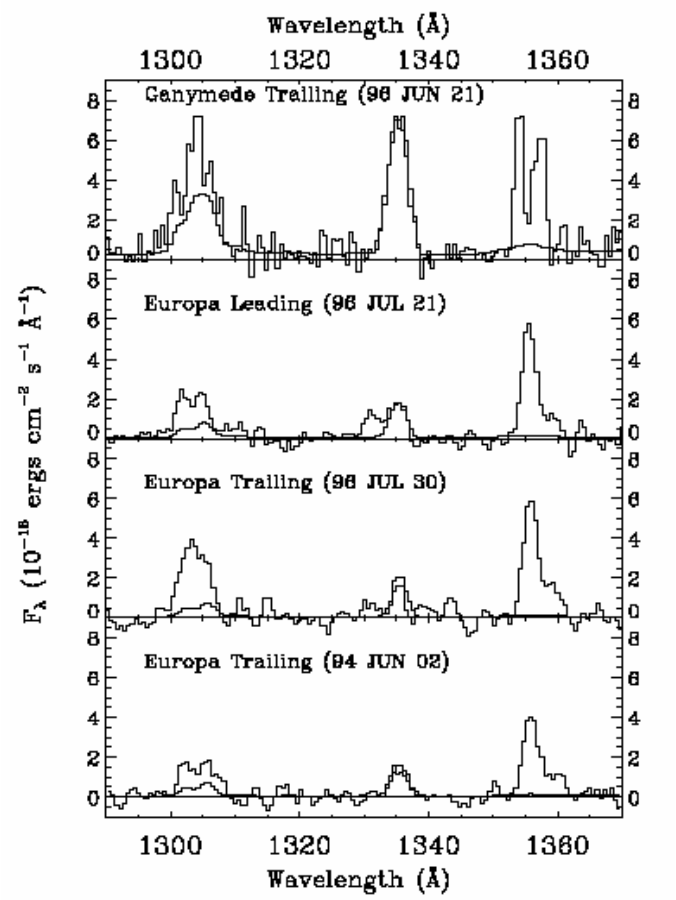

Figure 1. *The Hall et al. (1995, 1998) detections of electron excited oxygen emission at 1304 and 1356 Å from Europa , which provided the first direct evidence of an O_2 atmosphere on this satellite. The features at 1335 Å are due to solar C^+ emission reflected from the surface of the satellite. The dark line histogram shows a modeled reflected light component fit to the 1335 Å feature and assumed to be constant with wavelength [Figure 1 of Hall et al. 1998].*

Two additional sets of GHRS observations were obtained in July 1996 one from the leading hemisphere, and an additional set from the trailing hemisphere (*Hall et al*., 1998). All three of the GHRS spectra are shown in Figure 1, and the observed line fluxes are tabulated in

Table 2. With a finite scale height and emission above the limb included, the inferred molecular oxygen column densities are in the range ~(2.4-14) x 10^{14} cm^{-2}. Hall et al. noted that these observations were consistent with no atomic oxygen, and they set 3σ upper limits on the atomic oxygen abundances of (1.6 – 3.4) x 10^{13} cm^{-2}.

In 1999, observations of Europa's trailing hemisphere were obtained using the HST Space Telescope Imaging Spectrograph (STIS) using the long slit (52´´ x 2´´) and grating G140L, covering the wavelength range 1150 – 1720 A (*McGrath et al.,* 2004). Two images were obtained in each of 5 HST orbits spanning 7 hours, with the exception of the second exposure in the 2nd orbit, which failed. Detailed information about the individual exposures is given in Table 1 of *Cassidy et al.* (2007). The data format, illustrated in Figure 3, shows the type of information available in these data: monochromatic images of Europa in emission lines of HI Lyman-α 1215.67, OI 1304, CII 1335, and OI 1356, as well as a disk integrated spectrum of the satellite, which is directly comparable to the previous and subsequent observations.

Figure 4 shows the summed, monochromatic images in HI Lyman-α and oxygen, as well as a representative visible light image of the corresponding hemisphere of Europa. The HI Lyman-α and OI 1304 images have had the geocoronal background (process (1)) subtracted off. The Europa signal in the Lyman-α image consists of solar Lyman-α photons reflected from the surface of the satellite (process (2)). The 1304 Å image consists of both emission from Europa's oxygen atmosphere (processes (4) and (5)), and solar 1304 Å oxygen emission reflected from the surface of Europa (process (2)), which is difficult to subtract from an image due to its unknown spatial distribution. As shown in Figure 2, and discussed later in section 2.2 with regard to Cassini observations, the contribution of reflected light at 1304 Å does not dominate, but is non-neglibible. By contrast, the reflected component at 1356 Å is negligible because the sun does not produce OI 1356 Å line emission, so this image includes only emission from the atmosphere of

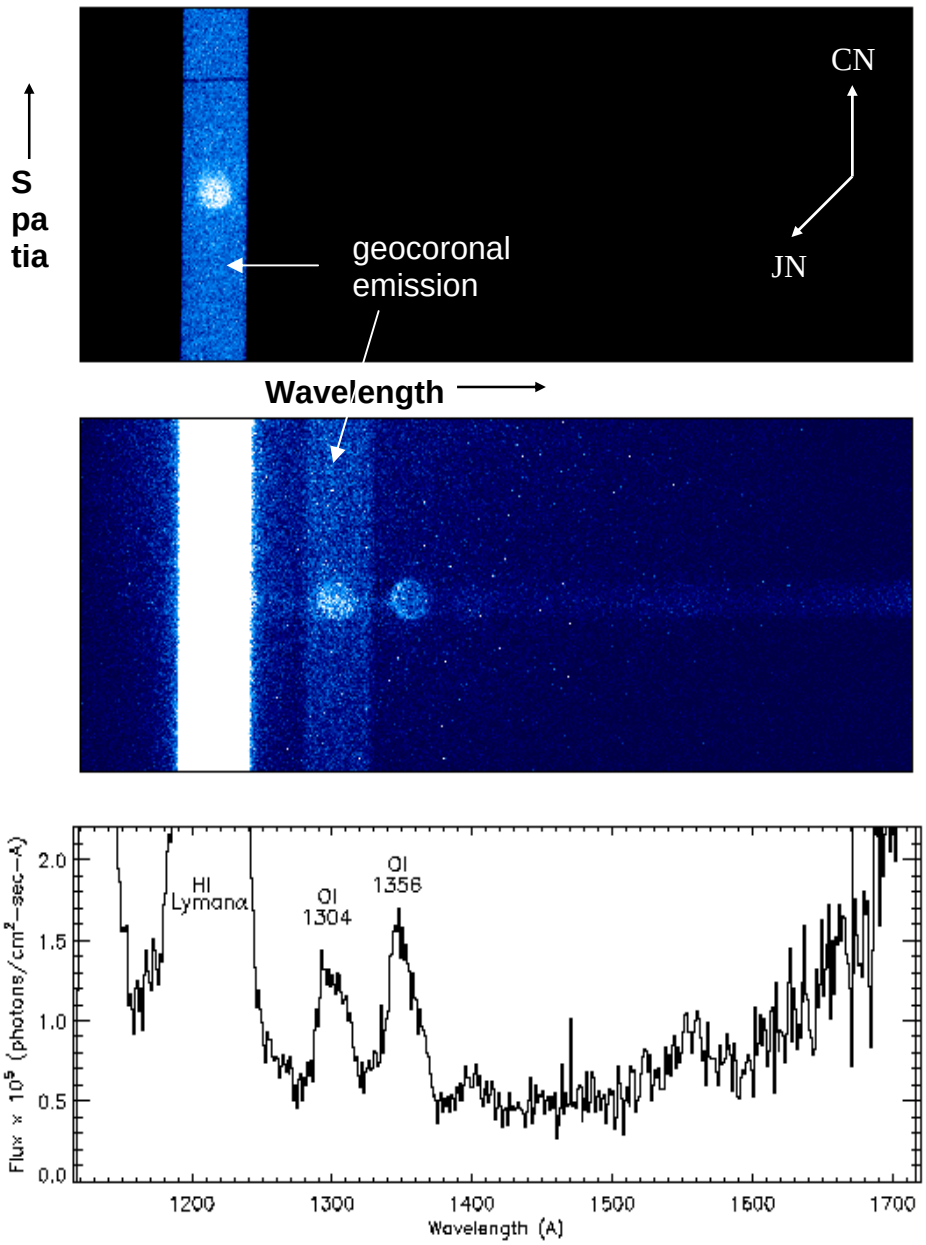

Figure 3. *Observation of Europa obtained in 1999 using the HST STIS, illustrating the data format. The top and middle panels are identical data displayed with a different stretch to emphasize Europa at HI Lyman-a wavelength (top) vs the oxygen emissions (middle). Emission filling the long slit at HI Lyman-a and OI 1304 is from process (1). The one-dimensional spectrum in the bottom panel is obtained by summing over the spatial rows corresponding to Europa in the middle panel. CN = celestial north; JN = Jovian (and Europa) north*

Europa. The OI 1356 image shown in Figure 4b has a signal to noise ratio (S/N) of only ~3 in the brightest regions. Figure 4b also shows that the OI 1356 emission peaks within the disk, and not in a ring of emission at the limb of the satellite, as would be expected from plasma interaction

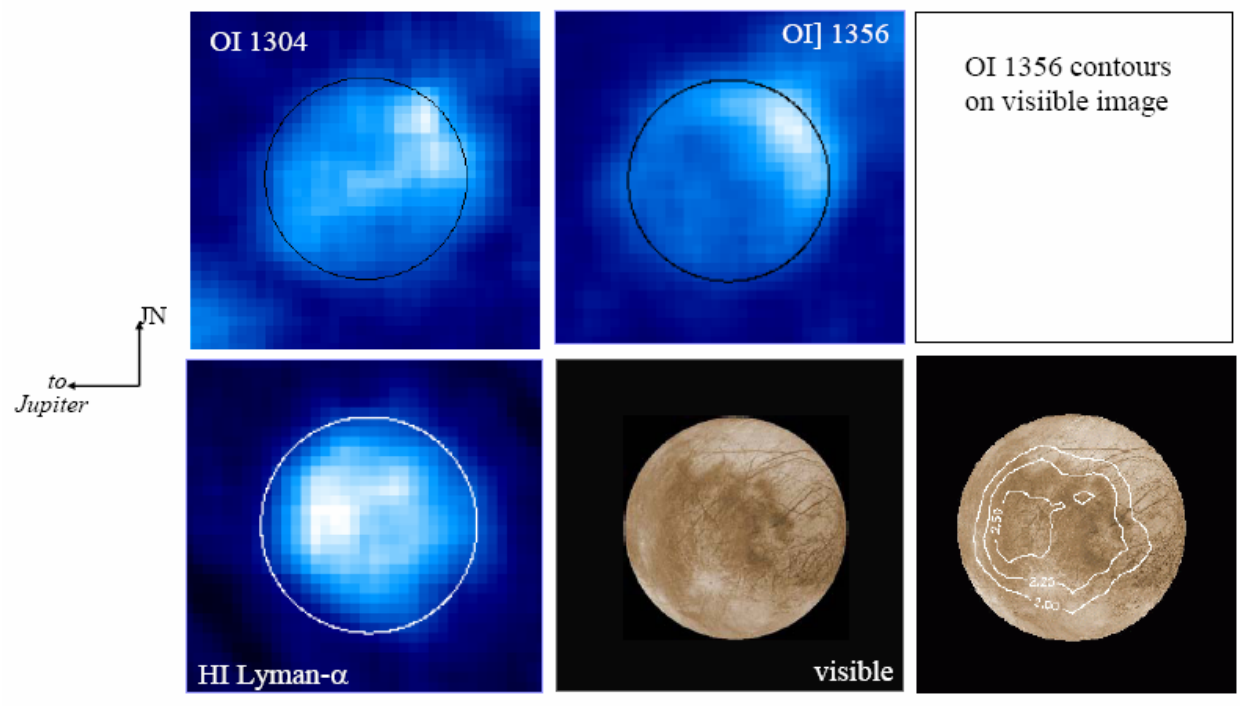

Figure 4.

with an optically thin atmosphere. It does display the expected limb glow around the limb, but includes a brighter region on the anti-jovian hemisphere. Prior to the acquisition of these images, *Saur et al*. (1998) published a detailed model of the plasma interaction at Europa, including a prediction of the morphology of the OI 1356 Å emission. Their prediction compared with the observation is shown in Figure 19.10 of *McGrath et al.* (2004); the prediction shows the brightest region off the limb of the sub Jovian hemisphere (opposite of that observed) and near the equator.

The observed brightness is an integral along the line of sight of the neutral density, the electron density, and an electron temperature dependent excitation rate coefficient. A localized bright region there has to be caused by either non-uniform plasma effects (n_e, T_e) exciting the emissions, or non-uniform density of the sputtered neutral gas. It is difficult to understand why the brightest region is on the disk because of the reduced path length there. Since Europa has a weak induced magnetic field (*Kivelson et al.*, 1997) it seems unlikely that it could focus jovian

electrons or energetic ions with finite gyroradii to sputter molecules into localized regions. The observation of localized O emission may suggest that the surface is not icy everywhere, but rather that the composition varies considerably with longitude, consistent with visible images and compositional data from Galileo. Figure 4b shows the 1356 Å brightness contours superposed on the corresponding visible image, indicating that the 1356 Å brightness may be correlated with the visibly bright regions. *Cassidy et al.* (2007) have explored the possibility of non-uniform sticking of O_2 as an explanation for the emission morphology. One caution concerning this interpretation is that the long integration time for the summed images shown in Figure 4 limits the ability to distinguish between the possibilities of a spatially variable source/loss process or local variability of the plasma exciting the emission. are The integration spans 7 hours, over more than half of a Jupiter rotation, during which time local plasma conditions, and therefore the emission morphology, might be expected to change significantly due to the undulation of the plasma sheet associated with the tilted jovian magnetic field. In fact, although the region of the surface observed does not change significantly over the 7 hour duration of the observations, the emission morphology does appear to vary, as shown in Figure 5 where the individual images that were summed to produce Figure 4 are shown. Unfortunately, these images have very low S/N ratio of only ~1 in the brightest regions, so caution is needed to avoid overinterpretation. However, if the variation is real, it would tend to argue against interpretation of the bright region on the anti-Jupiter hemisphere as being associated with the corresponding bright visible region on the surface. One thing to note is that the brightest emission is always in the anti-Jovian hemisphere, even though it appears to vary in latitude from north to south between images. As noted by *McGrath et al.* (1999) and *Ballester et al.* (2007), there is not a straightforward correlation between the variation of the location of the emission with the orientation of the background Jovian magnetic field, as is the case for similar plasma

excited emissions on Io.

Figure 4f shows the HI brightness contours superposed on the visible image. Simple inspection of the images shows an apparent correlation between the Lyman-α bright regions and the dark visible regions. This is likely due to surface albedo variations. The bright visible regions are thought to be composed of purer water ice, which is very dark at UV wavelengths, darker than most non-ice species (*Hendrix and Hansen* 2007) so it is expected that more Lyman-α is reflected from the surface in the visibly darker surface regions that in the visibly brighter regions.

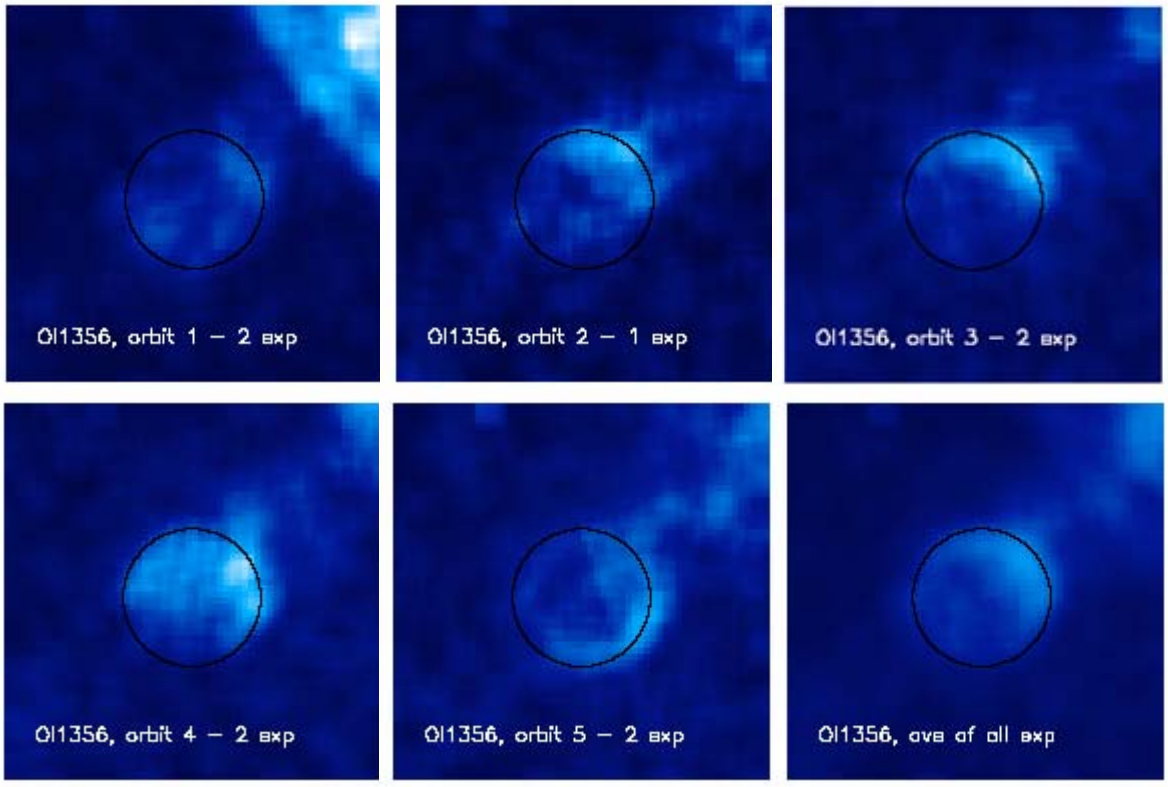

Figure 4.

A new and exciting result has recently been presented by *Retherford et al.* (2007) based on the latest HST observations made in February 2007 in conjunction with the New Horizons fly by of Jupiter. A new technique, using the Advanced Camera for Surveys (ACS) with the solar blind channel (SBC), was used to acquire a far-ultraviolet (FUV) oxygen emission image while

Europa was in eclipse. This image shows a bright region on the disk at northern latitude in the sub-jovian hemisphere, and an extended bright region extending off the disk which *Retherford et al.* interpret as wake emission. This tends to further support interpretation of the UV emission morphology as due to plasma, and not surface, effects.

2.2 Cassini Observations

Observations of the Galilean satellites were acquired by the Cassini spacecraft in December 2000 and January 2001 when it flew by Jupiter on the way to its primary orbital mission at Saturn. Much of the best satellite data were lost when the spacecraft entered safe mode a week before closest approach, however, two UltraViolet Imaging Spectrograph (UVIS) observations of Europa were acquired in the week following closest approach. The objective of these observations was to confirm the *Hall et al.* (1995) detection of a tenuous oxygen atmosphere and to compare these data, acquired at different times and for different orbital geometries, to the HST results.

Europa data pertinent to the atmosphere were acquired with the UVIS far-ultraviolet (FUV) channel (1115 – 1914 Å) on 6 and 12 January 2001. Details about the observations are given in Table 1. Further details, including graphical representations of the slit orientations for the two observing dates, are given in Table 1 and Figure 1 of *Hansen et al.* (2005). The UVIS, like the HST STIS, has a 2-dimensional detector which collects up to 1024 spectral pixels and 64 spatial pixels. For the Europa observations, the spatial pixels subtended 1.0 mr, and the spectral pixels 0.25 mr, while the slit width was 1.5 mr. Europa subtended 0.28 mr on January 6, and 0.20 mr on January 12, meaning it was essentially a point source in both the spatial and spectral dimensions for both observations. Because Europa was bore-sighted for the Cassini ISS camera, and the FUV channel is offset 0.37 mr from the ISS boresight, Europa was not centered in the slit for the observations, which results in a slight wavelength shift of the emission lines in the

spectral direction, and causes Europa to span spatial rows 31 and 32 in both observations. The total duration of the January 6 observation was 17,000 sec, in seventeen 1000-sec integrations, while the January 12 observation collected forty-one 1,000 sec images. The observation geometries from Cassini were quite different than the view available to earth-based telescopes because Europa was observed at greater than 90° phase angle, and portions of both the leading and trailing hemispheres, and sunlit and night sides, of Europa were included on both observing dates. The UVIS slit was oriented perpendicular to Jupiter's equatorial plane for both observations. On January 6 Europa was on the night side of Jupiter in its orbit, while on January 12 it was on the day side of Jupiter, near the ansa of its orbit as seen from Cassini, and it was tracked from the far side of its orbit, around the ansa to the near side over the duration of the observation.

Figure 6a shows the full UVIS FUV channel spectrum acquired on 6 January 2001 before the data were filtered and the fixed pattern signature (flat field) correction applied, and Figure 6b shows a 200 Å segment of this spectrum centered on the oxygen emissions. The non-oxygen emissions present in the full spectrum were from the Io plasma torus. The individual lines of the 1304 Å triplet at 1302.2, 1304.9, and 1306.0 Å and the 1356 Å doublet at 1355.6 and 1358.5 Å were all resolved in the UVIS spectrum, consistent with observation of a point source in the spectral direction, as noted above. Fig. 6c shows the flat-fielded spectrum for row 32 with a decomposition of each of the oxygen components of the spectrum. Figure 6d shows that once all the contributions to the data are modeled the remaining peaks are the combined signal from Europa's oxygen atmosphere and reflected sunlight from Europa's surface. The 1335 Å reflectance feature is marginally detected above the background. The solar reflection component at 1335 Å enabled determination of the albedo of Europa at 94º phase angle and subsequent calculation of the contribution of reflected sunlight to the 1216 Å, 1304 Å, and 1356 Å features,

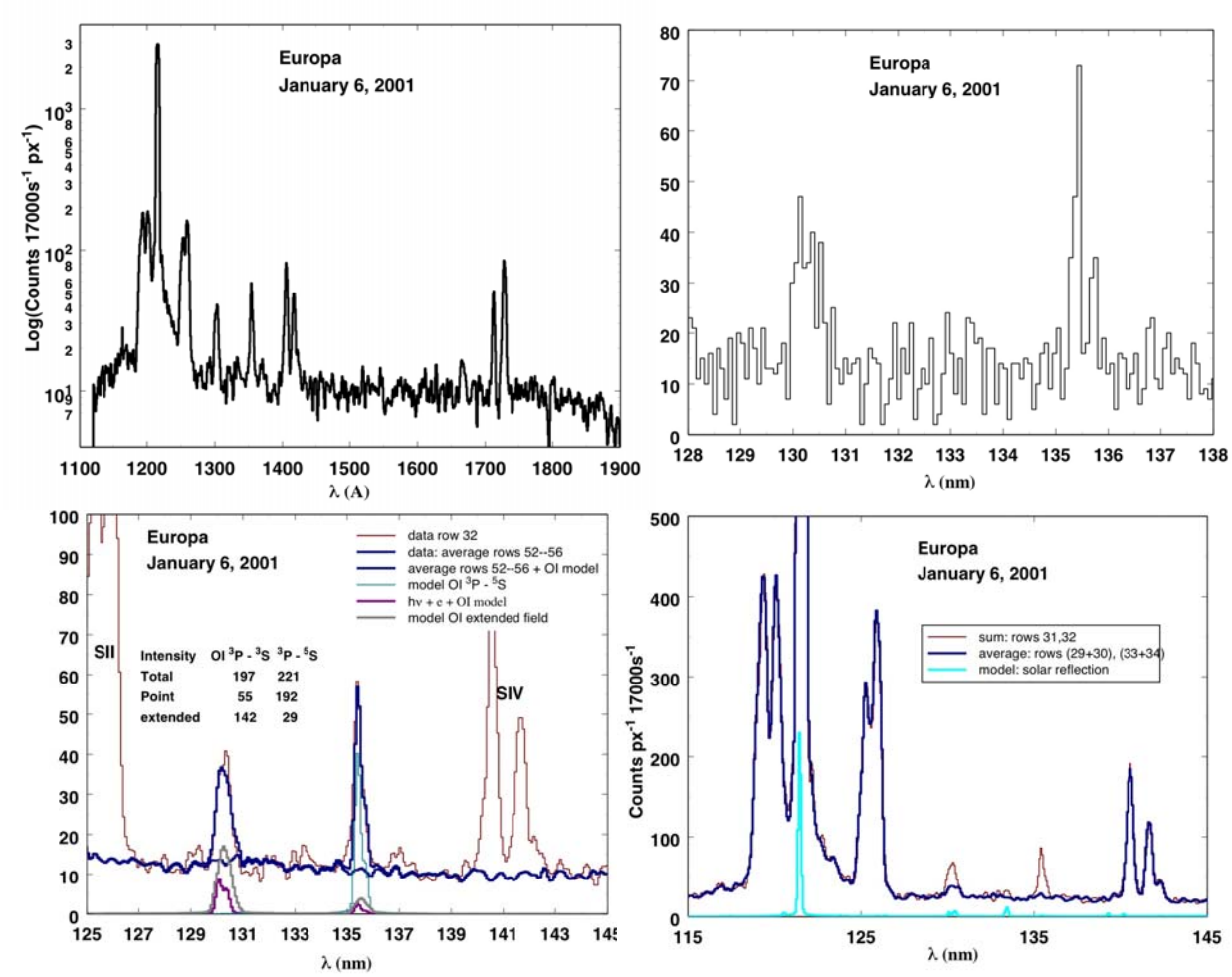

Figure 6. ***(a)*** *Full UVIS FUV raw spectrum acquired on 6 January 2001.* ***(b)*** *200 Å portion of the spectrum from (a) showing the resolved oxygen multiplets at 1304 and 1356 Å.* ***(c)*** *Spectrum of Europa (row 32), along with the derived components. The breakdown of point and spatially extended line components is shown quantitatively on the plot and in plotted simulated lines. Along the bottom of the plot the best-fit model predicts for Europa oxygen emission features are shown.* ***(d)*** *Spectrum from average of rows 29, 30, 33, 34 (blue line) superposed on the Europa spectrum (rows 31 and 32) (red line), showing the contribution of Io plasma torus emission (dark blue lin). The Europa spectrum (red line) shows the oxygen flux from Europa's sunlit surface and atmosphere at 1304 and 1356 Å.*

as illustrated in Figure 6d. The 1335 Å feature was used to determine an albedo of ~1% at 94º phase angle (compared with values of 1.3-1.6% from the HST observations), and account for the reflected solar light contribution to Europa's spectrum at 1216, 1304 and 1356 Å, assuming the albedo is flat throughout this region of the spectrum. Subtraction of the reflected light leaves the signal due solely to Europa's atmosphere. Since Europa was well away from the Io torus at the

time of the January 12 observation the analysis was simpler for that data. Atomic and molecular oxygen abundances derived from Cassini data are tabulated in Table 3. These are derived values, based on the flux observed at the instrument. Assumptions that go into these derived values include the scale height of the atmosphere, and the electron energy and density. *Hall et al.* (1998) derived a molecular oxygen vertical column density of (2.4 – 14) x 10^{14} cm^{-2}. Cassini molecular oxygen abundances fall within this range. The error bars on the Cassini measurements are ± ~15%.

A point source provides the best fit to the shape of the 1356 Å emission feature, consistent with a bound, near-surface O_2 atmosphere with scale height of ~200 km (assuming a temperature of 1000K). Once the 1356 Å feature was fit, the abundance of molecular oxygen and its contribution to the 1304 Å feature could be calculated. The remaining flux at 1304 Å was then attributed to the resonant scattering of sunlight by atomic oxygen (process 3), and electron excitation of atomic oxygen (process 4). Although somewhat subjective, the spectrum was best fit by including ~2% atomic O in the (point source) bound O_2 atmosphere, plus an extended tenuous atomic oxygen component overfilling a pixel. The *Hall et al.* (1995, 1998) would not have been able to identify an extended O component, since Europa filled most of the field of view of the GHRS slit, whereas Europa subtends less than one spatial pixel in the UVIS slit, thus more of the surrounding space is measured, enabling the UVIS detection of the extended atomic oxygen component. The spatial capability of UVIS was used to determine the oxygen profile as a function of distance from Europa. Figure 7a shows the distribution of oxygen in the January 6 data set and Figure 7b the January 12 data set as a function of spatial row. An extended oxygen component is apparent in both sets of observations. The 1356 Å feature is sharply peaked at row 32. The diffuse 1304 Å feature persists across all the illuminated spectral pixels and is detectable in rows 28, 29, and 30. Although the low spatial resolution prevents determination of

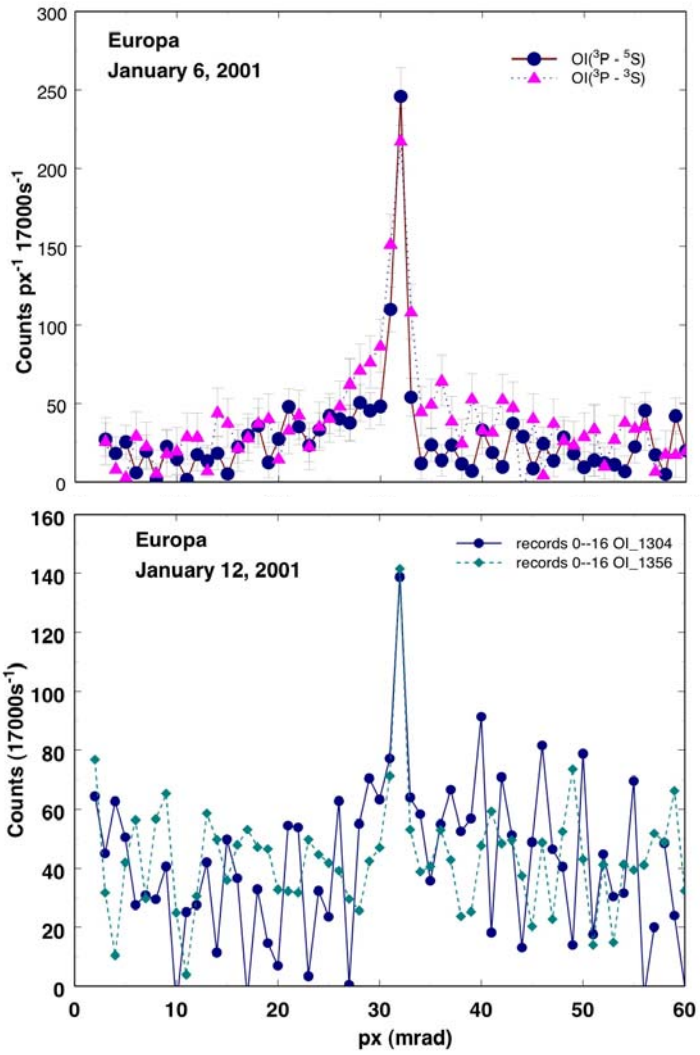

Figure 7. *The distribution of the 1304 Å and 1356 Å oxygen emission along the slit in the spatial direction. (a) In the 6 Jan 2001 data the 1356 Å feature is sharply peaked at the position of Europa, while the diffuse 1304 Å feature source persists across all the illuminated spectral pixels and is detectable in row 28, which corresponds to the opposite side of Europa's orbit. (b) The oxygen line emissions for the first 4.7 hrs of the January 12 data set are shown. Most of the January 12 data set was collected near the ansa of Europa's orbit as seen from Cassini. Both 1304 Å and 1356 Å are sharply peaked at Europa's position. One spatial pixel = 10 R_E.*

the size of the diffuse extended atmosphere, and any potential asymmetries such as suggested by *Burger and Johnson* (2004) for Europa's sodium cloud, the atomic oxygen cloud appears to be at least two pixels in extent, or ~ 22,000 km (~14 R_E) at Cassini's range.

The density of oxygen in Europa's extended atmosphere is 12 to 31 atoms cm^{-3}, at the points in time and space that Cassini observations were acquired. The detection of atomic

oxygen as an extended atmosphere adds a new observational constraint to models of the erosion of Europa's surface and life cycle of its atmosphere in the Jovian environment, such as those developed by *Saur et al.* (1998), *Shematovich and Johnson* (2001), and *Shematovich et al*. (2005).

3. IONOSPHERE

In simple terms, an ionosphere is a layer of plasma produced by photo- and/or particle impact ionization of a neutral atmosphere. In deep space planetary missions, ionospheres are detected by transmitting a one (or two)-way radio signal from the spacecraft to Earth (and back) through the atmosphere of the object of interest along a trajectory that produces an occultation of the spacecraft as seen from Earth. Such an occultation produces both an inbound and an outbound measurement of the target's ionosphere. In these radio occultations, a time series of signal strength and frequency are produced, and via comparison with a time series of predicted frequency computed from a precise spacecraft ephemeris a set of frequency residuals is derived. The residuals are inverted using standard techniques to obtain the refractivity, which is directly related to electron density, thereby providing an electron density profile vs altitude above the surface of the object. As of 2001, the Galileo mission had provided four radio occultations of Europa, in orbits E4, E6 (two) and E26. The geometries and results from three of these have been published by *Kliore et al.* (1997) and are shown in Figure 8. In addition, the E26 fly by resulted in a non-detection on the entry occultation and a detection on the exit occultation (*Kliore et al.*, 2001). The results of the 8 inbound and outbound measurements include five strong detections, one weak detection, and two non-detections of the ionosphere. The maximum electron densities of $\sim 10^3 - 10^4$ cm^{-3} occur at or near the surface of Europa with a plasma scale height of ~200 km below 300 km, and ~400 km above 300 km altitude. Assuming likely candidate constituents such as H_2O, O_2, H, H_2, OH and O leads to an estimated neutral density of order 10^8 cm^{-3}, and a

column density of order 10^{15} cm^{-2} assuming a neutral scale height of ~100 km.

The E4 entry detection geometry is looking toward the upstream direction of the plasma flow through the wake, where densities could well be higher. The non detection in the E6a exit occurred near the middle of the downstream wake region, and the E26 entry occultation non detection was at high latitude in the wake region. The wake region is shielded from the preferred direction of the plasma flow, which is toward the trailing hemisphere centered at 270 W longitude, and the electron densities there might be expected to be depleted. Also, according to the plasma model of *Saur et al.* (1998), the ionosphere can become detached from the satellite in this region. However, *Kliore et al.* (2001) also conclude, on the basis of the various geometries and detections, that a necessary condition for the detection of Europa's ionosphere may be that the trailing hemisphere is at least partially illuminated, which may indicate that the primary ionization source is solar photons as opposed to magnetospheric plasma electrons.

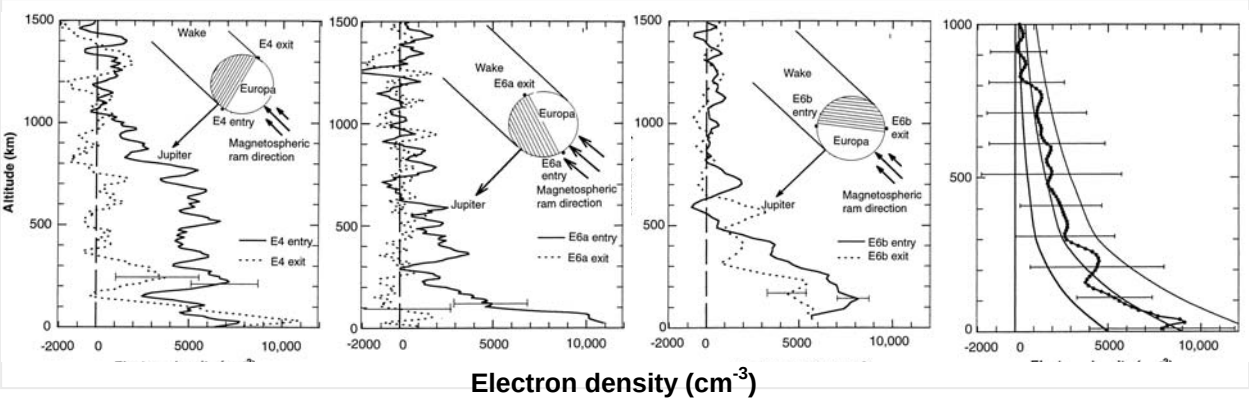

Figure 8.

On the other hand, *Saur et al.* (1998) found that electron impact ionization can generate Europa's ionosphere at the electron densities measured by *Kliore et al.* (1997). Using magnetospheric plasma conditions at Europa typical of the Voyager epoch (ne = 38 cm^{-3} and 2 cm^{-3} at Te = 20 eV and 250 eV, respectively) the electron impact ionization rate is 1.9 x 10-6 s^{-1}, while a solar maximum photoionization rate is 6 x $10^{-8}s^{-1}$. Given the intrinsic time constants

associated with these processes (6 and 190 days, respectively, compared with a 3.6 day orbital period), the diurnally averaged solar photoionization rate would be a factor of ~2 lower, whereas electron impact ionization depends mostly on ambient magnetospheric plasma densities. In order for photoionization to be competitive with electron impact ionization, the magnetospheric electron density would have to be ~ 1 cm^{-3}. For the Europa radio occultations observed in Galileo orbits E4 and E6, the ambient magnetospheric ion densities were ~25 and 15 cm^{-3}, respectively (*Paterson et al.,* 1999); the corresponding electron densities would be about 50% larger. *Kurth et al.* (2001) suggested a typical torus electron density of 80 cm^{-3} at the orbit of Europa. It is therefore very difficult to understand why the existence of an ionosphere should depend on solar illumination.

A further puzzle concerning Europa's ionosphere is the lack of an ionospheric signature in complementary Galileo particles and fields measurements collected in the wake region during the E4 flyby (*Gurnett et al.,* 1998; *Paterson et al.,* 1999). Because ionospheric plasma should presumably be convected downstream, these measurements should have detected plasma densities commensurate with the electron densities inferred by *Kliore et al.* (1997, 2001). *Gurnett et al.* (1998) found electron density enhancements of only 50-100 electrons cm^{-3} at Europa during the E4 flyby. If the peak density of *Paterson et al.* (1999) were interpreted as O_2^+, then the ion (and electron) density is at most ~100 cm^{-3}. Furthermore, *Kurth et al.* (2001) reported plasma wave observations for the nine Galileo spacecraft close flybys of Europa. The maximum density enhancement observed on any flyby was on the E15 flyby when the electron density jumped from 200 to 400 cm^{-3} as the spacecraft entered the wake.

In summary, while the existence of an ionosphere at Europa is well established, its origin and characteristics are still very poorly understood.

4. MINOR SPECIES, NEUTRAL CLOUDS, AND TORUS

With the exception of atomic oxygen, discussed above, the other minor species associated with Europa have been observed at distances well above the surface, where there is no overlap with detections of the primary atmospheric species O_2 (see Figure 1). Minor species in Europa's atmosphere can aid in investigation of surface composition and also serve as a proxy for mapping the distribution of the major atmospheric species far from the surface. The minor species detected to date include sodium, potassium, and some form of hydrogen (atomic or molecular). Numerous sets of observations exist of sodium, but only a single set of observations each has been made of potassium and hydrogen.

4.1 Sodium and Potassium

The first detection of sodium (Na) from Europa was made on 5 June 1995 (see Table 1) when 10 long-slit spectra covering 5883 – 5904 Å were obtained at the 1.53m University of Arizona telescope on Mt. Bigelow with total integration time of 4.33 hours (*Brown and Hill*, 1996). The long slit was oriented perpendicular to Europa's orbital plane, and emission intensity along the slit in the N-S direction from Europa was derived (top panel of Figure 9). No variability was observed among the 10 spectra, so they were all co-added for analysis. Emission from the Na D_1 and D_2 lines at 5895.92 and 5889.95 Å, respectively, was detected with an intensity ratio of 1.70 ± 0.05, consistent with the value of 1.66 expected for optically thin emission from resonant scattering of sunlight by Na in Europa's vicinity. The line of sight column density is therefore directly proportional to the emission intensity. The detected brightness and line of sight column density vs radial distance in the N-S direction from Europa is shown in Figure 9. Note that a factor of 2 calibration error was later found in these published data, so the values along the y axes in the top panel of Figure 9 need to be multiplied by 2. The emission is seen to be symmetric about the satellite in the N-S direction out to ~$10R_E$, and then is slightly brighter in the N than the S from 10-20 R_E. The emission intensity inside ~5 R_E cannot

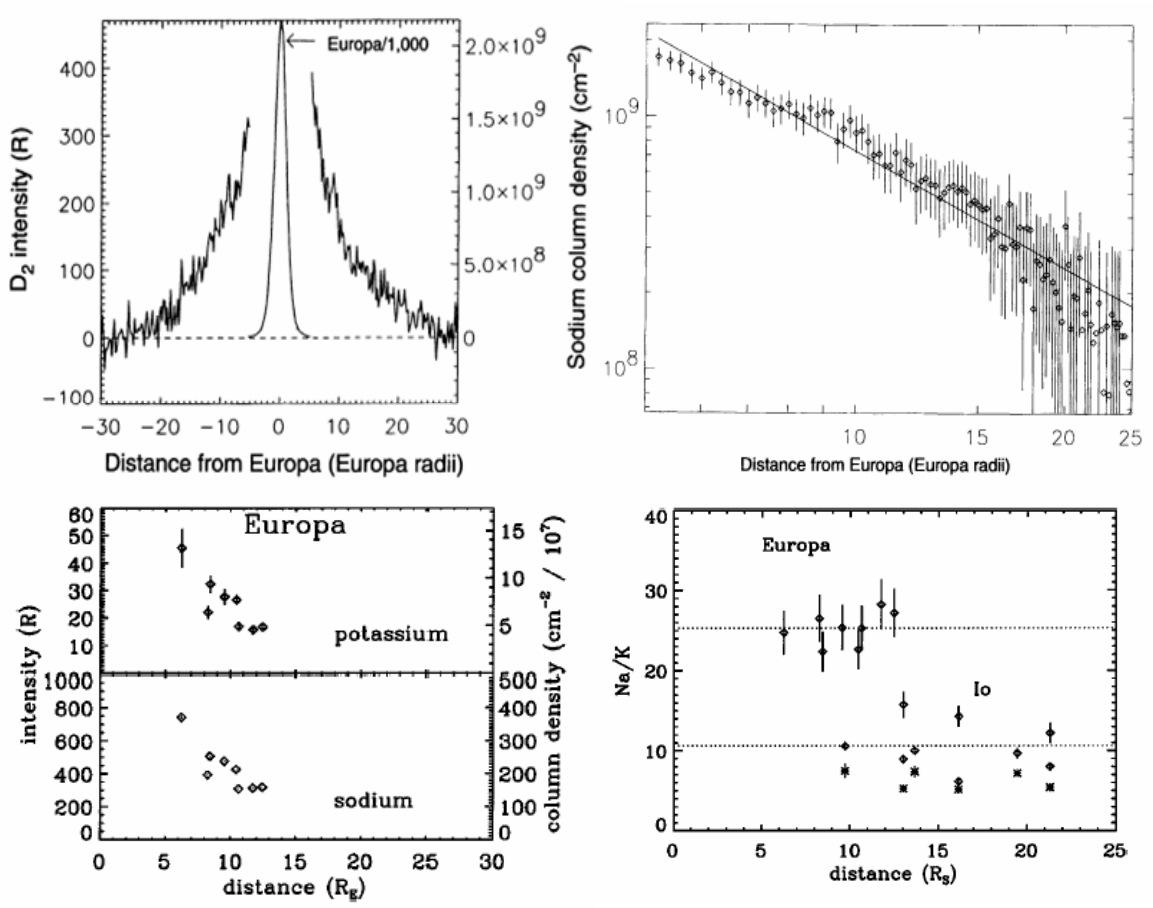

Figure 8. Na and K at Europa

be determined because of the overwhelming brightness of the Europa continuum. The sodium emission is detectable out to ~25 R_E, which requires that Na atoms leave the surface with $v > 2$ km s^{-1}, and that most of the particle velocities are this large or larger to account for the flatness of the profile between 5 and 10 R_E. Since sublimation at the surface temperature of 95 K would produce velocities of only 0.3 km s^{-1}, *Brown and Hill* concluded that the most likely source mechanism is sputtering by energetic magnetospheric particles. The total mass of sodium implied by the distribution shown in Figure 9 is 840 kg, and extrapolation of the profile to the surface implies a surface density of ~100 cm^{-3}, which is 300 times less than the closely bound molecular oxygen atmosphere.

A second set of high-resolution, ground-based spectroscopic measurements were made

on 9 Sept 1998 using the HIRES instrument on Keck (*Brown* 2001). The Na observations were repeated, but this time simultaneous measurements were also made of the potassium doublet at 7664.90 and 7698.96 Å. The long slit was oriented perpendicular to Europa's orbital plane, and centered at several different positions east of the satellite. The intensity profile obtained was very similar to that from the *Brown and Hill* (1996) observations (bottom panel Figure 9). On 15 Nov 1998 an identical set of observations were made of Io. These measurements showed that the Europa Na/K ratio of ~25 is both very different from that at Io (Na/K~10), and very different from a meteoritic source or the solar abundance ratios (*Brown*, 2001; *Johnson et al.,* 2002). Iogenic sodium implanted into Europa's surface ice was originally suggested as the source of the sodium, however, this idea was later revised based on the detection of potassium, and the measured ratio of Na/K for Europa compared to Io, and an endogenic source is now favored (see following chapter by Johnson et al.)

Four subsequent sets of Na observations were obtained in 1999 and 2000 (see Table 1). The orbital geometry of Europa for these four sets of observations is shown in Figure 10, illustrating which parts of the Na cloud are observed on each occasion. Observations on 28

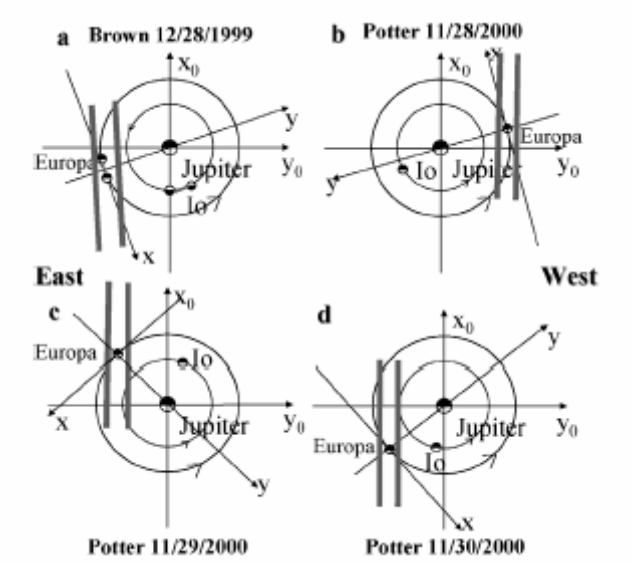

December 1999 were made with the identical setup as *Brown* (2001) using the Keck HIRES instrument, and are reported in *Leblanc et al.* (2002). In this set of observations, the first attempts were made to obtain detailed maps of the Na emission morphology near Europa. Six sets of scans were made: N-S and E-W sets centered on Europa; E-W sets at 10 R_E north and south of Europa; and E-W sets at 20 R_E north and south of Europa. The consolidated Na intensity information from these scans is shown in Figure 11. This more complete set of measurements

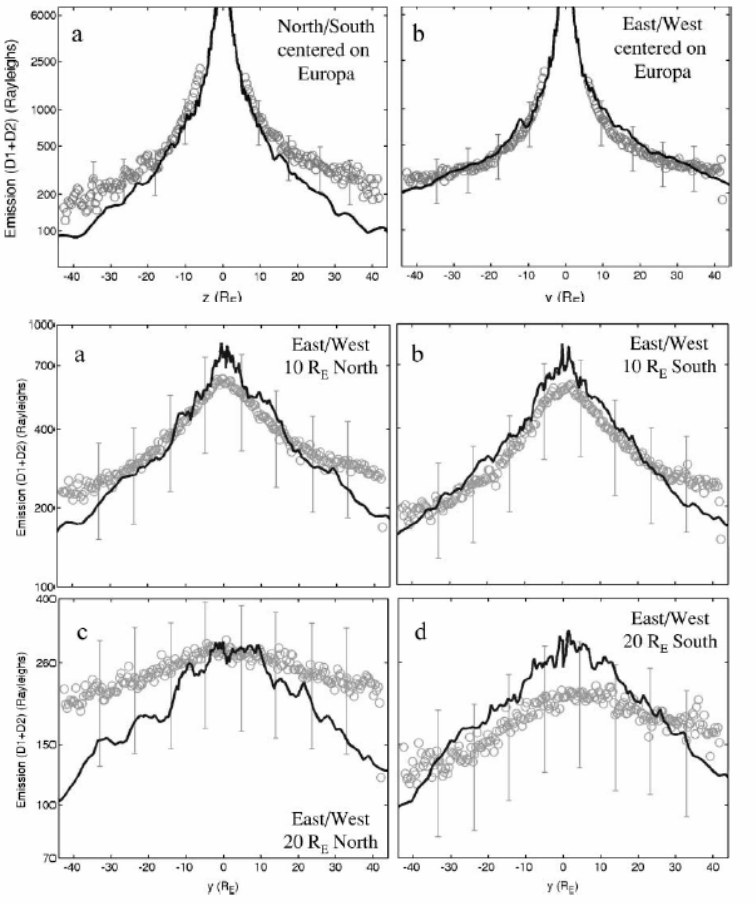

Figure 11.

clearly shows that the Na cloud asymmetries are different in the direction perpendicular to the orbital plane (N-S) than in the direction parallel to the orbital plane (E-W). The observed emission morphology is again symmetric, both N-S and E-W, within ~ 10 R_E, but then, as with the 1995 observations, somewhat brighter north of Europa than south at d > 10 R_E. However, the

overall emission intensity is approximately twice as bright in these 1999 observations than in the 1995 and 1998 observations, and substantial variations in emission intensity at given locations (e.g., 20 R_E north and south of Europa, see Figure 10) are seen during the course of the observations.

Three additional sets of Na observations were obtained in November 2000 using the McMath-Pierce Solar Telescope at Kitt Peak National Observatory (*Leblanc et al.,* 2005) . In these observations, the Na emission was sampled in 1''x 1'' regions centered at 2'' and 3'' from the center of Europa in all of N, S, E, and W directions on 28 Nov 2000; and at 2'', 3'' in N, S, E, and W directions and 4'' N, E, and W on 29 and 30 Nov 2000. The mapping locations for the 29 and 30 Nov 2000 observations are illustrated in Figure 12. Whereas earlier observations had not been obtained closer than 5 R_E, these 2000 observations obtained measurements as close as ~3.5 R_E. Table 2 of *Leblanc et al.* (2005) provides a detailed compilation of the observed Na intensities at different locations for the four sets of 1999 and 2000 observations. The differences

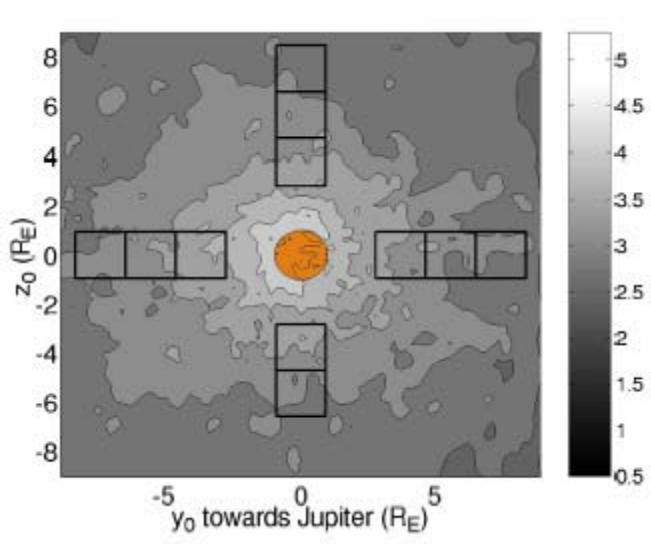

Figure 12.

in intensities show that within 2-3" of Europa, there is a leading/trailing asymmetry that *Leblanc et al.* (2005) contend is dominated by the production of atmospheric Na from the trailing

hemisphere, and also depends on the solar flux. They also contend thata N-S brightness asymmetries correlate with the centrifugal (magnetic) latitude of Europa, but this is based on only a handful of data points.

A final set of (possible) Na observations add an interesting potential link between the plasma electron excited oxygen emissions and the resonant fluorescent Na emissions just described. A set of Cassini ISS clear filter images obtained on 10 January 2001 while Europa was going into eclipse (*Porco et al.,* 2003) is shown in Figure 13. In these images, there appears to be a bright region in the northern sub-jovian hemisphere that persists well after Europa is completely in shadow. *Porco et al.* noted that Jupiter light reflected from Ganymede is

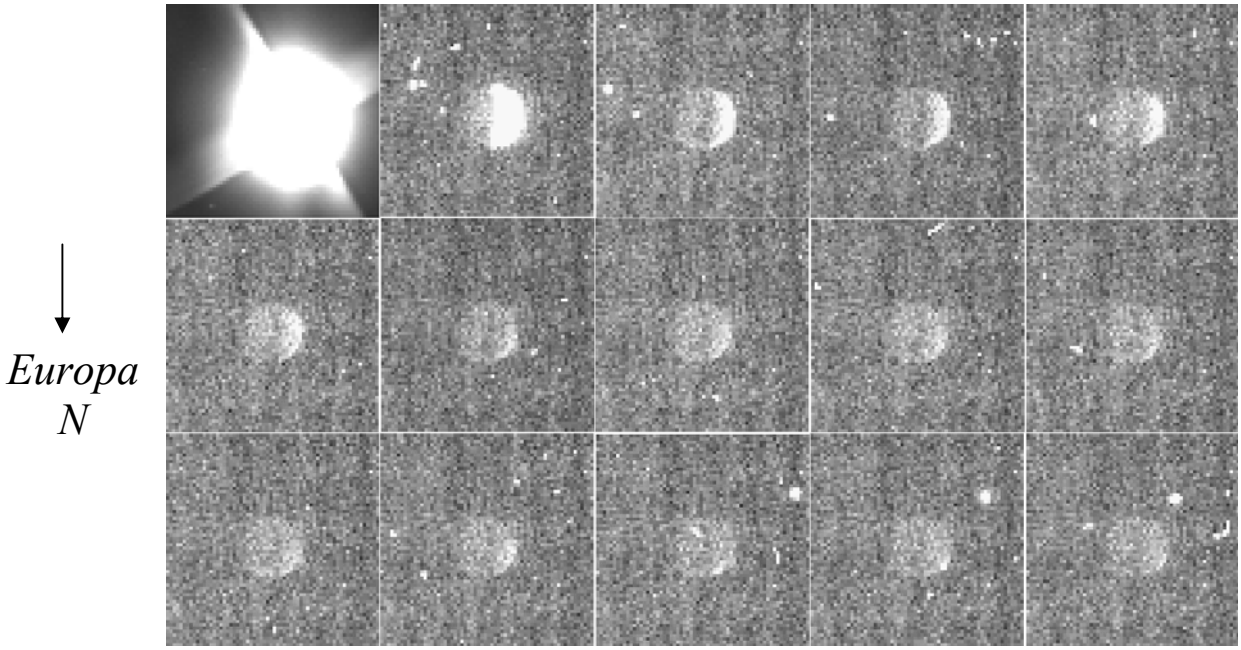

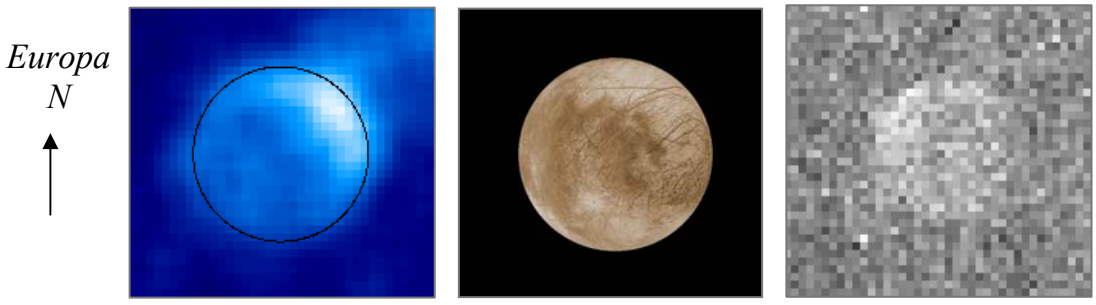

OI 1356
L=257

Visible
L=257

Cassini clear filter
in eclipse
L=253

Figure 9.

a potential illumination source, but non-uniform bright emission on the Jupiter facing hemisphere would be inconsistent with such an origin. Serendipitously, the hemisphere captured in these images is almost identical to that of the HST/STIS images shown in Figure 4. Although the vantage point and orbital phase are very different for Cassini compared to HST, both sets of observations were viewing the trailing, plasma-bombarded hemisphere. The two sets of images both show enhancements in the northern hemisphere, but the Cassini emission is in the sub-jovian northern quadrant, while the HST emission is in the anti-jovian quadrant. Obviously, because the Cassini images were acquired while Europa was in eclipse, resonant fluorescence of sunlight is not a possible source. By analogy with similar images of Io acquired by the Galileo SSI (Geissler reference), it has been suggested that the emission in these images may be produced by electron impact excitation of atomic Na in Europa's atmosphere (Cassidy *et al.,* 2008). Although the S/N ratio in these images is low, the new observation of O emission from Europa in eclipse (*Retherford et al.,* 2007) with a somewhat similar morphology lends credence to the reality of the emission seen in the Cassini eclipse images. These images, along with the variation seen in the O emission morphology shown in Figure 5, tend to support the interpretation that the various morphologies seen for both the (potentially) electron excited Na and oxygen emissions are caused by variations in the plasma and its interaction with Europa, rather than non-uniform surface properties of the satellite, or localized sputtering sources or sinks as have been put forward by *Cassidy et al.* (2007, 2008).

4.2 Europa Torus

As Cassini approached Jupiter, the Ion and Neutral Camera (INCA), which is a channel of the Magnetospheric Imaging Instrument (MIMI), was used to acquire a 15-hr Energetic Neutral Atom (ENA) image of the Jupiter system beginning on 1 January 2001 when Cassini

was at a distance of 140 R_J (Figure 14). ENAs are produced by charge exchange between neutral atoms and magnetically trapped energetic ions. Bright features were noted in the ENA image on both sides of Jupiter, peaking just outside Europa's orbit at a distance of ~9.5 R_J (*Mauk et al.,* 2003). *Mauk et al.* interpreted their image as a torus of neutral atoms centered on the orbit of Europa. When magnetically trapped energetic protons in the Jupiter system collide with a neutral atom in such a torus, charge exchange ionizes the neutral atom and neutralizes the

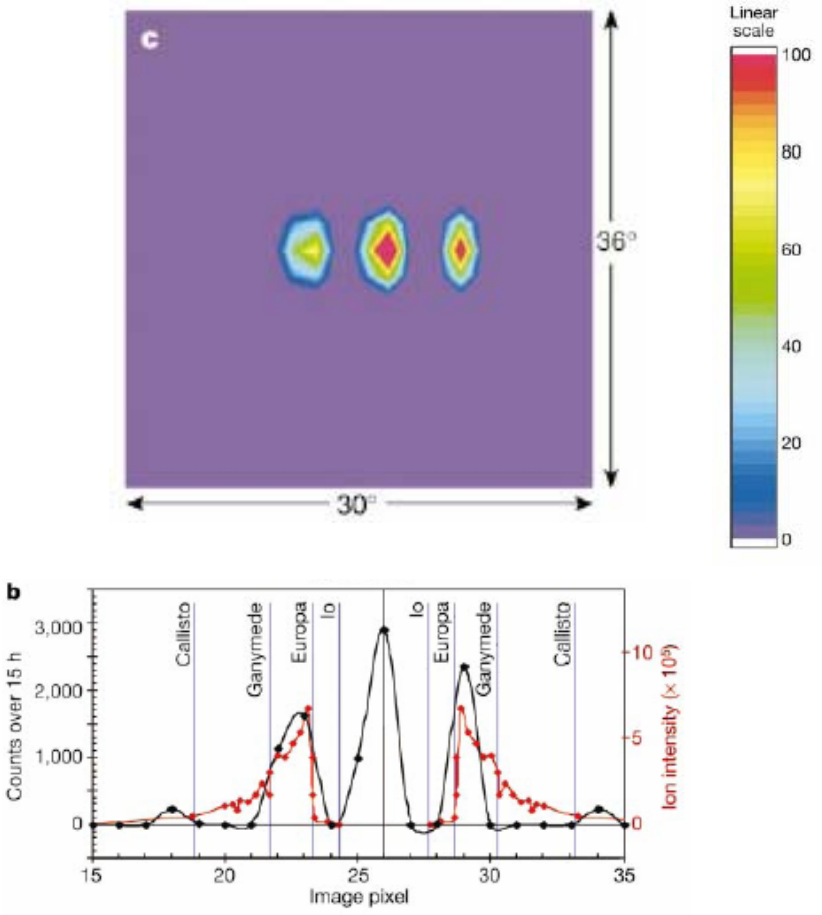

Figure 10. *Top: INCA image (in counts, with the scale on the right hand side)of Jupiter and Europa from Mauk et al. (2003) showing an edge-on view of a torus of neutral material (most likely hydrogen) just outside the orbit of Europa. Bottom: The top 2-d image collapsed along the vertical axis and plotted as the black line with the intensity of protons, energy-integrated from 50 to 80 keV, plotted in the red line. The orbits of the Galilean satellites are indicate with vertical lines. [From Figures 1 and 2 of Mauk et al. 2003]*

original proton, which then leaves the system. The INCA observations cannot distinguish the composition of the original target neturals. The most likely constituents available for charge

exchange in the vicinity of Europa are the products of its sputtered water ice surface and oxygen atmosphere: H_2O, H, H_2, O, OH and O_2. The INCA data are consistent with an emission region with a radial extent and height of 1-5 R_J, symmetric about Europa's orbit, and a total content of ~9 x 10^{33} particles. Assuming a torus radius of 2 R_J gives a density of ~40 particles (atoms or molecules) cm^{-3}. This interpretation is corroborated by the Galileo Energetic Particle Detector (EPD) instrument measurement of a depletion of energetic particle flux in the vicinity of Europa's orbit (*Lagg et al.,* 2003).

The atomic oxygen in the Europa's extended atmosphere is subject to ionization and loss, from photoionization, charge exchange, and electron dissociation. The rate of ionization from these three processes is ~1.6 x 10^{-6} per sec, thus the lifetime for an oxygen atom in Europa's exosphere is estimated to be 7.2 days. In theory enough oxygen atoms are lost from Europa's atmosphere to account for the total number required by *Mauk et al.* as neutral species distributed in the magnetosphere. In order to put upper bounds on oxygen in the Europa torus *Hansen et al.* (2005) analyzed data from a February 2001 outbound Cassini UVIS observation. For this observation the UVIS slit centered on Jupiter and aligned parallel to Jupiter's equator (see Figure 6a of *Hansen et al.,* 2005), and the total integration time is ~28 hr. During the observation the boresight was slewed slowly from north to south every 30 minutes, so that the total integration time is ~7 hr in any particular direction. Figure 6b of *Hansen et al.* (2005) shows a 2-dimensional plot of these data. Atomic oxygen emission from the Io torus is evident, but there is no atomic oxygen emission at the position of Europa. If oxygen is a contributor to the torus identified by *Mauk et al.* its density must be below levels detectable by UVIS. The density that UVIS could have detected is ~8 atoms/cm^3, a factor of 5 less than the value postulated by *Mauk et al.* for a torus radius of 2 R_J. This suggests that the torus is substantially more extended, possibly out to the 5 R_J considered by *Mauk et al.*, or that it is composed of H and/or H_2.

5. VARIABILITY

The multiple observations described above and summarized in Table 1 afford an opportunity to assess, to a limited extent, the degree of variability in Europa's atmosphere and neutral clouds. The major difficulty is our limited ability to derive meaningful atmospheric neutral abundances (via, e.g., equation because of our scant knowledge about the properties, including variation, of the magnetospheric plasma in the vicinity of Europa. All the observed emissions are an integral along the line of sight, and virtually all inversions of the brightness to derive column densities to date assume a uniform value for electron density and temperature. The only detailed forward modeling to date, by *Saur et al.* (1998), has not been successful in reproducing the oxygen emission morphology. It is important to bear this limitation in mind while considering what solid information can be gleaned from the observed variability.

There are 6 sets of observations of the O_2 atmosphere by HST and Cassini, four sets of radio occultations of the ionosphere, and six sets of Na observations taken at different orbital, solar illumination, and magnetic geometries, including multiple observations with roughly the same orientation taken at different times. There are also two observations of the Europa torus, albeit one a non-detection. We consider each in turn.

The disk-averaged spectroscopic line fluxes for OI 1304 and 1356 for both the HST and Cassini observations, both the observed fluxes and fluxes normalized to a common distance, are given in Table 2. The observations from Table 1 have been numbered, and are referenced by number in Table 2 and in the discussion that follows. HST has observed Europa's dayside, leading hemisphere once (obs #2), its dayside trailing hemisphere 3 times (obs #1,3,4), and its dayside hemisphere in eclipse twice (obs #7,8). Disk average line fluxes are not available for the latter two observations. Two of the trailing hemisphere observations (obs #1,3) were performed in an identical manner separated by a little over two years; the third trailing hemisphere observation

(obs #4) was performed with a different instrument, but the line fluxes derived from it should be directly comparable to the other two. There is no significant variation in either the disk integrated OI 1304 or 1356 line flux between obs #1 and 3, but a factor of ~2 brightening of both of these between obs #(1,3) and #4 acquired over 3 years later. *Hall et al.* (1995) noted that *"*Some caution is needed in interpreting the factor of two difference in trailing hemisphere flux from HST/GHRS measurements. During the first HST orbit, the telescope was aligned so that Europa was centered in the aperture; however, during the third orbital exposure, the telescope boresight drifted ~0.8 arcsec from this initial orientation. This drift means that much of Europa's disk may have been excluded from the aperture, possibly artificially depressing detected emission intensities." Since the oxygen atmosphere is widely accepted to be sputter generated, and the observed emissions are also excited by the plasma, the observed variability seems more likely to be caused by plasma variability than by significant changes in the surface properties of Europa that would affect the sputtering source, unless a currently undetected phenomenon such as surface geysers or surface outgassing are operative. Variability of emission morphology over a 6.5 hr interval also appears to be present in the 1999 HST observations (Figure 5) although the low S/N ratio hampers the interpretation.

The Cassini observations of Europa were at significantly different orbital locations than the HST observations, on the solar (obs #6) and roughly anti-solar (obs #5) sides of Jupiter. As with the HST observations, there is a significant variation of the oxygen emission between the two Cassini observations. This is illustrated Figure 15, where the difference between the January 6 and January 12 data sets is clearly evident. As can be seen from Table 2, the line fluxes decreased by a factor of 3 in the 6 days between the observations. In order to explore the variability due to viewing geometry, *Hansen et al.* (2005) calculated the emission using the electron environment presented by *Saur et al.* (1998). The Saur *et al* model features a steady-

state distribution of electron energies around Europa, with plasma flowing in on one side and creating a cavity on the other, producing non-uniform excitation of the oxygen. At the time of the January 12 observation UVIS was looking at the leading side of Europa, at a wake region depleted of electrons. The UVIS observations are qualitatively consistent with the Saur *et al.* model, however only a factor of ~1.6 difference in brightness can be attributed to the difference in leading vs. trailing side electron density and electron energy with the Saur model, vs. the 3x difference in flux observed. Using the Saur model for the spatial distribution of electrons and accounting for the viewing geometry, molecular oxygen abundances of 7.4 x 10^{14} cm^{-2} on January 12 and 12.4 x 10^{14} cm^{-2} on January 6 were calculated. The spectra show no indication of a variable OI 1356 intensity on Jan. 12 over an 11.4 hr time interval (see Figure 5 of *Hansen et al.,* 2005), which discounts an electron environment variability associated with the Io torus wobble. An increase in oxygen abundance between January 6 and January 12 might be indicative of a transient event, but the significant decrease between the two observations is

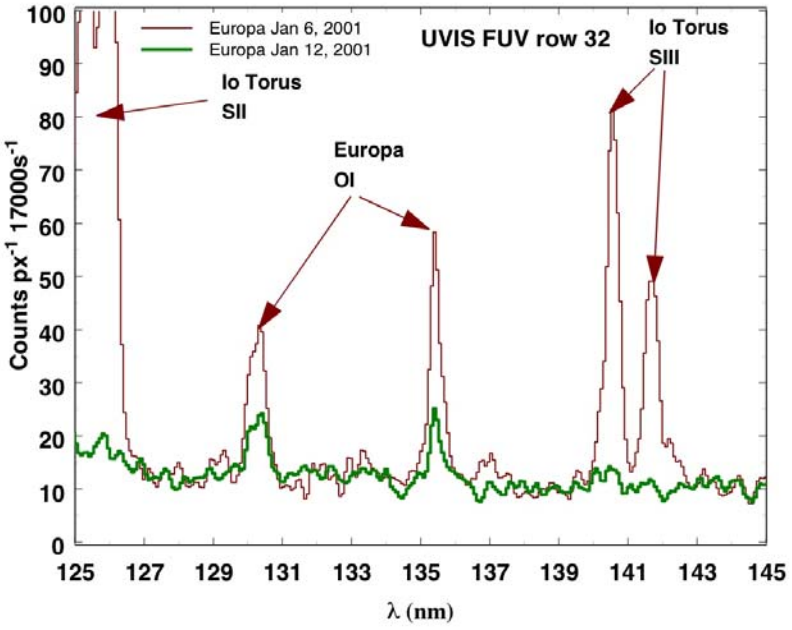

Figure 15. *Comparison of January 6 and January 12, 2001 exposures with the flux from the latter reduced by a factor of ~3. With Europa at the ansa of its orbit as seen from Cassini, Io's torus was not within the UVIS field of view on January 12.*

harder to explain as a transient phenomenon. The more likely explanation is a change in the plasma environment such as reported by *Frank et al*. (2002).

It is also interesting to compare the Cassini observations with the HST observations. HST obs #1 and Cassini obs #5 captured Europa at almost identical orbital phases (= the same plasma bombardment orientation) but viewed from different directions. Cassini saw the flank of the plasma flow (30deg toward the leading hemisphere), with the half toward the plasma flow being sunlit and the downstream half (with respect to the plasma flow) in darkness, while HST saw the trailing sunlit hemisphere. In this comparison, the less sunlit and less bombarded hemisphere has twice as much flux at 1356 A. HST obs #2 and Cassini obs #6 saw the same hemisphere of the satellite at very different orbital phases. In this case, HST saw the leading (downstream) sunlit hemisphere, while Cassini saw the leading (downstream) hemisphere with half in sunlight and half in darkness, and the HST 1356 A flux is about 30% larger. It is tempting, as with the ionosphere observations, to try to associate higher fluxes (densities) with sunlight, however, with only a few data points this is little more than idle speculation. As mentioned briefly in section xx, the variation in emission morphology seen in the six consecutive HST 1356 images shown in Figure xx, for which the sunlight, bombardment and orbital position change very little over the course of the observations, argues fairly strongly against the emission enhancement in the anti-jovian hemisphere being associated with surface effects such as locally enhanced sputtering or preferential sticking in visibly dark surface regions, and in favor of variation of the plasma associated with the wobbling of the background jovian magnetic field, as has been seen at Io. However, as pointed out by *McGrath et al. (1999)* and *Ballester et al.* (2007), unlike at Io, there is not a straightforward correlation between the emission morphology and the change in background field orientation.

The ionosphere observations show a range of levels of detection, including two non-detections, the E6a exit (obs #10) and the E26 entry (obs #12). It's interesting to note that the E4 ionosphere occultation occurred for a Europa geometry (orbital, sunlight, plasma bombardment) that is nearly identical to that for HST obs #4 (shown in Figures 4 and 5), except Cassini is looking toward the upstream direction, while HST is looking toward the downstream direction. This is the HST observation that shows the brightest 1356 A emission region in the anti-jovian hemisphere, which corresponds to the E4 exit measurement that shows a very weak, low scale height electron density profile (left panel of Figure 8). The geometry (orbital, sunlight, plasma bombardment) for the E6a radio occultation is nearly identical to Cassini obs #6. The E6a entry profile is along the ram direction, which may explain the compressed, low scale height nature of this profile, whereas the E6a exit profile is along the middle of the wake, and is a non-detection. This Cassini observation corresponds to an oxygen density at the low end of the range observed in the six sets of observations. Finally, the E6b exit profile is over the longitude (256deg W) at the center of the HST obs #4 images shown in Figure 4, where there is no obvious 1356 emission.

The variations seen in the Na observations are complex, and have been explored in detail in *Leblanc et al.* (2005). One interesting conclusion they draw is that the total emission intensity from one measurement to another cannot be explained solely by the differences in the geometry of observations, and it is likely that there was a significant variation in the source rate from 11/28/2000 to 11/30/2000. This is a rich dataset which is continuing to be exploited with on-going investigations and modeling (e.g., xxxx 2007 AGU abstract). The current thinking concerning the variations seen closest to the satellite is described further in the next chapter (see *Johnson et al.* next chapter, Figure 2).

5. SUMMARY: OUTSTANDING ISSUES AND FUTURE WORK

Although substantial progress has been made in characterizing the bound atmosphere, neutral clouds and torus of Europa in the past 14 years since the first detection of oxygen, the data continues to be very sparse. As for Io, the detection of related atmospheric products will be important in understanding Europa's atmosphere, and a better understanding may come only when other atmospheric species are detected. For instance, a substantial though transient H_2O sublimation atmosphere will be present in the equatorial regions when the subsolar point is over the icy leading hemisphere but may be absent when the subsolar point is over the trailing hemisphere, which is likely dominated by water of hydration. Such variability will affect the ionosphere. In addition, since the surface materials are decomposed by radiolysis a large number of products other than O_2 and H_2 should be present, like the sodium and potassium components discussed above. CO_2 has been detected in the surface ice (*Smyth et al.* 1998) and appears to be correlated with the dark terrain on the anti-jovian and leading hemispheres (*Hansen et al.* 2007). Although the CO_2 band depth is comparable to that measured at Callisto, no measurement of CO_2 in vapor form has been made at Europa, as at Callisto. *Hansen et al.* (2007) suggest an internal, sub-surface ocean source of the surface CO_2. Searches for CO_2 and its products (CO, C) should be performed at Europa in future. Given that the CO_2 atmosphere on Callisto has not been detected remotely, detections may be difficult to accomplish by remote sensing. Techniques such as those currently being used on Cassini - including mass spectrometers, and detailed plasma characterization – as well as high resolution IR spectroscopy for identification of surface constituents, would be useful tools on future missions to Europa or the jovian system.

Interpretation of the observations is also hampered by the lack of understanding of the local plasma environment, and its variability, at Europa. Further in situ characterization is critical because, unlike Io, the plasma near Europa is too tenuous to be observed with current ground-based and Earth orbit techniques. Until further data is obtained, continued work on detailed

interaction models such as those of Saur et al. and Shilling et al. are indispensible in trying to make further progress interpreting the data already in hand. There is also additional worthwhile work to be done on the existing data. For example, all the GHRS spectra acquired by HST contain temporal information that has yet to be exploited. HST STIS is scheduled to be repaired during Servicing Mission 4 in 2008. Further observations of the oxygen emissions such as those shown in Figures 4 and 5 would be very useful. Additional HST UV observations using the ACS are also planned for 2008, and should help unravel the outstanding issues concerning the origin and variation of the emission morphologies seen in the existing HST and Cassini oxygen emissions. It would be helpful if HST observations could be done to confirm and/or extend the Cassini eclipse images shown in Figure 13.

Perhaps the best immediate route for progress is ground-based observing programs aimed at characterizing the Na and potassium clouds at Europa. Such observations are clearly feasible, and until further observations of the main constituents are obtained, Na and K serve as very useful proxies for understanding the surface/plasma source and loss processes operative at Europa.

6. REFERENCES

Broadfoot, A. L., M. J. Belton, P. Z. Takacs, B. R. Sandel, D. E. Shemansky, J. B. Holberg, J. M. Ajello, H. W. Moos, S. K. Atreya, T. M. Donahue, J. L. Bertaux, J. E. Blamont, D. F. Strobel, J. C. McConnell, R. Goody, A. Dalgarno, and M. B. McElroy (1979) Extreme ultraviolet observations from Voyager 1 encounter with Jupiter. *Science*, 204, 979–982.

Brown, M. E. (2001) Potassium in Europa's atmosphere. *Icarus*, 151, 190-195.

Brown, R. A. (1974) Optical line emission from Io. In *IAU Symp. 65: Exploration of the Planetary System,* pp. 527-531.

Brown, W. L., Augustyniak W. M., Lanzerotti L. J., Johnson R. E., and Evatt R. (1980) Linear and nonlinear processes in the erosion of H_2O ice by fast light ions. *Phys Rev Lett*, 45, 1632–1635.

Brown, M. E. and Hill, R. E. (1996) Discovery of an extended sodium atmosphere around Europa. *Nature*, 380, 229-231.

Brown, M. E. (2001) Potassium in Europa's atmosphere. *Icarus* 151, 190-195.

Burger, M. H. and Johnson, R. E., (2004) Europa's neutral cloud: morphology and comparisons to Io. *Icarus*, 171, 557-560.

Carlson R. W., Bhattacharyya J. C., Smith B. A., Johnson T. V., Hidayat B., Smith S. A., Taylor G. E., O'Leary B., and Brinkmann R. T. (1973) An Atmosphere on Ganymede from Its Occultation of SAO 186800 on 7 June 1972. *Science,* 182, 53–55.

Carlson R. W. (1999) A tenuous carbon dioxide atmosphere on Jupiter's moon Callisto. *Science*, 283, 821-821.

Cassidy, T. A., Johnson R. E., Geissler P. E., Leblanc F. (2008) Simulation of Na D emission near Europa during eclipse. *submitted to JGR.*

Cassidy, T. A., Johnson R. E., McGrath M. A., Wong, M. A., Cooper, J. F. (2007) The Spatial Morphology of Europa's Near-surface O_2 Atmosphere. *Icarus,* 191, 755-764.

Frank, L. A., Paterson, W. R., Khurana, K. K., 2002. Observations of thermal plasmas in Jupiter's magnetotail, JGR 107:A1, 10.1029/2001JA000077.

Gurnett, D. A., W. S. Kurth, A. Roux, S. J. Bolton, E. A. Thomsen, and J. B. Groene (1998) Galileo plasma wave observations near Europa. *Geophys. Res. Lett.*, 25, 237.

Hall, D. T., Strobel, D. F., Feldman, P. D., McGrath, M. A., Weaver, H. A., 1995. Detection of an oxygen atmosphere on Jupiter's moon Europa. *Nature,* 373, 677-679.

Hall D. T., Feldman P. D., McGrath M. A., Strobel D. F. (1998) The far-ultraviolet oxygen airglow of Europa and Ganymede, Astrophysical Journal 499, 475-481.

Hansen C. J., Bolton S. J., Matson D. J., Spilker L. J., Lebreton J. P. (2004) The Cassini / Huygens Flyby of Jupiter, *Icarus*, 172, 1-8.

Hansen C. J., Shemansky D. and Hendrix A. (2005) Cassini UVIS Observations of Europa's Oxygen Atmosphere and Torus. *Icarus,* 176, 305-315.

Hansen, G. B., McCord T. B. (2007) Widespread CO_2 and Other Non-ice Compounds on the Anti-Jovian and Trailing Sides of Europa from Galileo/NIMS Observations. Submitted to *GRL.*

Hendrix, A. R and Hansen, C. J. (2007) Ultraviolet observations of Phoebe from the Cassini UVIS, *Icaurs,* in press.

Johnson, R. E., Lanzerotti L. J., and Brown W. L. (1982) Planetary applications of ion induced erosion of condensed gas frosts. Nuclear Instruments and Methods in Physics Research A 198, 147–158.

Judge D. L., and Carlson R. W. (1974) Pioneer 10 Observations of the Ultraviolet Glow in the Vicinity of Jupiter. *Science,* 183, 317.

Judge D. L., Carlson R. W., Wu F.-M., and Hartmann U. G. (1976) Pioneer 10 and 11 ultraviolet photometer observations of the Jovian satellites. In *Jupiter*, ed. T. Gehrels, Tucson: University of Arizona Press, p. 1068.

Kivelson, M. G., K. K. Khurana, F. V. Coroniti, S. Joy, C. T. Russell, R. J. Walker, J. Warnecke, L. Bennett, and C. Polanskey (1997) Magnetic field and magnetosphere of ganymede. *Geophys. Res. Lett.*, 24, 2155.

Kliore, A., D. L. Cain, G. Fjeldbo, B. L. Seidel, and S. I. Rasool (1974) Preliminary Results on the Atmospheres of Io and Jupiter from the Pioneer 10 S-Band Occultation Experiment.

Science, 183, 323–324.

Kliore, A. J., G. Fjeldbo, B. L. Seidel, D. N. Sweetnam, T. T. Sesplaukis, P. M. Woiceshyn, and S. I. Rasool (1975) The atmosphere of Io from Pioneer 10 radio occultation measurements. *Icarus,* 24, 407–410.

Kliore A. J., Hinson D. P., Flasar F. M., Nagy A. F., and Cravens T. E. (1977) The ionosphere of europa from galileo radio occultations. *Science,* 277, 355–358.

Kliore, A. J., A. Anabtawi, and A. F. Nagy, The Ionospheres of Europa, Ganymede, and Callisto, EOS, abstract #P12B-0506 pp. B506+, 2001.

Kumar, S., Photochemistry of SO_2 in the atmosphere of Io and implications on atmospheric escape, J. Geophys. Res. 87, 1677–1684, 1982.

Kupo, I., Y. Mekler, and A. Eviatar, Detection of ionized sulfur in the Jovian magnetosphere, ApJ 205, L51–L53, 1976.

Kurth, W. S., D. A. Gurnett, A. M. Persoon, A. Roux, S. J. Bolton, and C. J. Alexander (2001) The plasma wave environment of Europa. *Planet. Space Sci.*, 49, 345–363.

Leblanc, F., R. E. Johnson, and M. E. Brown (2002) Europa's Sodium Atmosphere: An Ocean Source? *Icarus*, 159, 132.

Leblanc, F., A.E. Potter, R. M. Killen, and R. E. Johnson (2005) Origins of Europa Na cloud and torus. *Icarus*, 178, 367-385.

Mauk, B. H., Mitchell, D. G., Krimigis, S. M., Roelof, E. C., Paranicas, C. P., 2003. Energetic neutral atoms from a trans-Europa gas torus at Jupiter. Nature 421, 920-922.

McDonough T. R., and Brice N. M. (1973) A Saturnian Gas Ring and the Recycling of Titan's Atmosphere. *Icarus*, 20, 136.

McGrath M. A., Lellouch E., Strobel D. F., Feldman P. D., Johnson R. E. (2004) Satellite Atmospheres, Chapter 19 in *Jupiter: The Planet, Satellites and Magnetosphere,* ed. F.

Bagenal, T. Dowling, W. McKinnon, Cambridge University Press.

Paterson, W. R., L. A. Frank, and K. L. Ackerson (1999) Galileo plasma observations at Europa: Ion energy spectra and moments. J. Geophys. Res., 104, 22,779–22,792.

Pilcher, C. B., S. T. Ridgway, and T. B. McCord (1972) Galilean Satellites: Identification of Water Frost. *Science*, 178, 1087–1089.

Porco C. and 23 co-authors (2003) Cassini imaging of Jupiter's atmosphere, satellites, and rings. *Science*, 299, 1541

Saur, J., Strobel, D. F., Neubauer, F. M., 1998. Interaction of the Jovian magnetosphere with Europa: Constraints on the neutral atmosphere. *JGR* 103, 19947-19962.

Shematovich, V. I. and Johnson, R. E. (2001) Near-surface oxygen atmosphere at Europa. *Adv. Space Res.*, 27, 1881-1888.

Shematovich, V. I., Johnson, R. E., Cooper, J. F., Wong, M. C. (2005) Surface-bounded atmosphere of Europa. *Icarus*, 173, 480-498.

Trafton, L. (1975). Detection of a potassium cloud near Io. *Nature*, 258, 690–692.

Wu F.-M., Judge D. L., and Carlson R. W. (1978). Europa: Ultraviolet Emissions and the Possibility of Atomic Oxygen and Hydrogen Clouds. *ApJ,* 225, 325-334.

Yung Y. L. and McElroy M. B. (1977) Stability of an oxygen atmosphere on Ganymede. *Icarus*, 30, 97–103.